electronics

MDPI

Article

A High-Precision Positioning Method for Autonomous Underwater Vehicles with Communication Delays

Pei Li [1], Zongyao Li [1], Chaoyang Chen [1,*], Juan Chen [1] and Zuguo Chen [1,2]

[1] School of Information and Electrical Engineering, Hunan University of Science and Technology, Xiangtan 411100, China
[2] Shenzhen Institute of Advanced Technology, Chinese Academy of Sciences, Shenzhen 518055, China
* Correspondence: ouzk@163.com

Abstract: In underwater navigation of autonomous underwater vehicles (AUVs), communication delays frequently occur, leading to a reduction in positioning accuracy. To mitigate this challenge, this work introduces a novel method for relative angle correction, aiming to reconstruct measurement information. Initially, Doppler measurement data are assimilated into the reconstruction of measurement equations to determine the relative angle between the AUV and the observatory. Subsequently, the obtained angle information is integrated into the Extended Kalman Filter (EKF) for the reconstruction of measurement equations. The proposed method effectively reduces positioning errors caused by hydroacoustic communication delays, consequently enhancing AUV positioning accuracy. The efficacy of the proposed method is demonstrated through a simulation study. Simulation results reveal that the incorporation of Doppler angle correction in the reconstructed measurement information method significantly decreases the localization error by approximately 50% compared to EKF and by around 20% compared to the method lacking angle correction.

Keywords: AUV; communication delay; Extended Kalman Filter; Doppler measurement

Citation: Li, P.; Li, Z.; Chen, C.; Chen, J.; Chen, Z. A High-Precision Positioning Method for Autonomous Underwater Vehicles with Communication Delays. *Electronics* **2024**, *13*, 466. https://doi.org/10.3390/electronics13030466

Academic Editors: Olivier Sename, Xu Yang, Daxiong Ji and Chenglong Du

Received: 23 October 2023
Revised: 6 January 2024
Accepted: 17 January 2024
Published: 23 January 2024

1. Introduction

An Autonomous Underwater Vehicle (AUV), distinguished by its integration of intelligent technology and advanced computing prowess, emerges as a sophisticated underwater submersible. This marvel seamlessly incorporates a multitude of modular functions, including automatic control, precise navigation and positioning, energy conversion, target recognition, and fault management. It boasts an array of advantages, including remarkable autonomy, heightened stealth, broad environmental adaptability, cost-effectiveness, and effortless expandability. AUVs are now being used for a variety of tasks, including oceanographic surveys, demining, and bathymetric data collection in marine and riverine environments. And AUVs play a vital role in ocean information acquisition, requiring robust and reliable navigation performance [1,2]. For complex and dynamic marine environments, self-localization function of AUVs is the foundation for accomplishing potential applications [3]. At present, there are three main wireless communication methods: radio communication, optical communication and acoustic communication. Currently, the Global Navigation Satellite System (GNSS) stands as the fundamental system for high-precision land and air navigation [4]. Nevertheless, the radio signal experiences rapid attenuation in water, rendering GNSS inapplicable for underwater navigation [5]. Optical communication range is short and requires high-quality water. In our operational scenarios, underwater robots frequently demand long-distance communication in turbid waters. Consequently, optical communication with shorter latency is not particularly suitable for our specific context. Acoustic communication is the most effective method because of its slow attenuation speed and long transmission distance [6,7]. However, acoustic communication also has non-negligible limitations, including delay, path loss, limited bandwidth, multipath

and so on [8,9]. In practice, the propagation delay is related to the speed and distance of propagation [10]. The propagation speed of radio waves in air is equivalent to the speed of light. In contrast, underwater acoustics propagate slowly, resulting in communication delays when utilizing hydroacoustic communications for localization. The consideration of delay factors becomes crucial in underwater localization, bearing substantial research significance. Furthermore, due to the complexity of the underwater environment, there is still a gap between the navigation and positioning accuracy of underwater vehicles compared to those of air and land, and for the time being, underwater navigation has become an important issue in the field of AUV research, and the navigation and positioning of AUV are very challenging [11–15].

In underwater navigation missions, precise navigation information is the prerequisite for the aforementioned applications. Location data are not merely employed to determine spatial coordinates; they also constitute a critical safeguard for the overall effective utilization and secure retrieval of AUVs. Utilizing surface positioning robots such as unmanned boats and smart buoys, alongside the application of relative ranging information, offers an effective approach to calibrate AUV position data. This calibration process eliminates cumulative errors stemming from the AUV's own inertial guidance system, thus facilitating long-term accurate navigation and positioning for miniature AUVs [16]. Due to the significantly lower propagation loss of acoustic signals compared to radio signals, acoustic navigation emerges as the most effective method. This underscores the essential role of hydroacoustic positioning systems as an indispensable component for localization and navigation in automatic underwater vehicles (AUVs). They represent a pivotal key to the successful execution of underwater navigation missions [17,18]. In addition, the challenge of striking a balance between the robustness of the control system and the utilization of communication resources equally demands consideration [19]. For instance, Du et al. [20] addresses an improved co-design method of dynamical controller and asynchronous integral-type event-triggered mechanisms (ETMs) for a class of linear systems with external disturbances and measurement noises. A tradeoff can be achieved between the robustness of the control system and the occupancy rate of communication resources.

The recursive state estimation is a typical problem of discrete-time dynamic systems, especially in state estimation for navigation system [21]. The Kalman Filter (KF) is a classic recursive estimation algorithm that divides the navigation process into state prediction and update [22]. Currently, there are a lot of KF variants aimed at optimizing the state estimation [23–26]. It is important to note that the traditional KF requires the system model to be linear. In practical applications, the relationship between state equations and observation equations established by the Kalman Filter is more prone to nonlinearity. This characteristic renders the traditional Kalman Filter algorithm inapplicable. [27]. Therefore, the Extended Kalman Filter (EKF) has been presented and has become the most widely used algorithm for AUV navigation and nonlinear navigation models [28]. For instance, in [29], a variational Bayesian-based Adaptive EKF algorithm is proposed for cooperative navigation of master–slave autonomous underwater vehicles (AUVs), improving the robustness of unknown or time-varying noises accordingly. Nonetheless, within the practical underwater navigation environment, underwater acoustic communications are limited by the following channel impairments: time variability, narrow bandwidth, multipath, frequency-selective fading [30]. The mutual communication between AUVs and other nodes, along with the processes of data handling and underwater data transmission, inevitably entail a specific duration. This results in a delay in information propagation underwater. When introducing delayed measurement information into the EKF filtering process, the resulting estimation outcomes can exhibit significant errors, consequently impacting the ultimate filtering effectiveness. Therefore, for the AUV localization problem under consideration, it is necessary to take the delay in information propagation underwater into consideration. This is the motivation of the current study.

In the current literature, prevalent strategies involve enhancing established localization models by integrating additional aids like Doppler Velocity Logs (DVL), etc., or pursuing

improved AUV localization through algorithmic refinements and debugging. Wang [31] proposed a single-beacon navigation method based on direct signal (DS) and surface reflection signal time delay (SRS), established a tracking model based on DS and SRS, smoothed the navigation results, and made an observational analysis. The accuracy analysis showed that the DS-SRS-based method has better navigation accuracy compared with the DS-based method. Xu [32] proposes a new robust delay filtering algorithm for cooperative localization of autonomous underwater vehicles (AUVs). The modified measurement equation of nonlinear cooperative positioning system with time-varying delay is derived. The delay caused by information processing and propagation of the underwater acoustic modem is converted into measurement deviation. Secondly, the statistical similarity metric (SSM) is introduced to construct a cost function to improve the robustness of the system to outliers caused by anomalies in hydroacoustic communication and Doppler velocity (DVL) measurements, and the proposed robust delay algorithm mitigates the effect of delayed measurements with outliers on localization accuracy. To solve the problem of DVL failure in AUV motion, Zhu et al. [33] proposes a hybrid prediction method combining the long-short-term memory neural network (LSTM) and a machine learning method-assisted adaptive filtering algorithm. The method can effectively solve the problems of DVL failure and the inability to provide measurement values and outlier interference in the DVL measurement process. Yan [34] designs two model-free proportional differential (PD) tracking controllers considering time-varying communication delays, and gives sufficient conditions for asymptotic stability. By using a linear matrix inequality (LMI) the relationship between controller gain and time delay is established, which could calculate an upper limit on the allowable time delay. Zhang et al. [35] construct an integrated navigation solution model based on the Extended Kalman Filter (EKF), which uses distance and velocity as measurement information, to reduce the navigation error due to underwater vehicle motion. Li et al. [36] propose a Bayesian inference algorithm for long-baseline acoustic localization of a maneuvering undersea vehicle, which compensates for vehicle motion during the interrogation-reception time interval between the vehicle and transponders of the LBL system using only acoustic timing measurements. Thomson et al. [37] develop a linearized Bayesian inversion algorithm for high-precision localization of an AUV on a test range using time difference of arrival acoustic data in a LBL positioning system. Bo Xu [38] deeply analyzed the broadcast cooperative navigation time delay error generation and action mechanism, and proposed a positioning method based on the measurement update. The method models the delay as a system state quantity, stores all the system state quantities during the filter operation, directly updates the delay information of the arrival measurement, and reconstructs a new filtering equation to realize the state filtering estimation, so as to improve the system accuracy. Yao [39] introduces the Decomposed Extended Kalman Filter (DEKF), necessitating the storage of all delay states before conducting filtering processes. In Reference [40], a technique for underwater acoustic communication and detection delay has been proposed.

Therefore, it is essential to propose a method that can effectively alleviate the positioning errors induced by underwater communication delays, thereby augmenting the precision of localization. This article addresses the issue of communication latency in underwater navigation systems. Building upon the research of AUV underwater navigation systems, it introduces Doppler measurement information to reconstruct measurement data. A refined EKF algorithm based on reconstructed measurement data is proposed. This approach proves efficacious in addressing the cumulative errors arising during the measurement process, thereby enhancing the precision of AUV positioning. Its effectiveness is evaluated through simulated experiments.

- To enhance the accuracy of AUV positioning, this work introduces the issue of communication delays during underwater positioning and analyzes its impact on EKF nonlinear filtering.
- To address the localization error induced by communication delay, we propose a localization compensation algorithm. This algorithm compensates for the localization information by reconstructing the measured data, resulting in a more accurate position.

- To optimize the reconstructed measurement information, we propose a Doppler-corrected angle method. This approach corrects the heading angle of AUV motion using Doppler measurement information, effectively mitigating the issue of cumulative angular errors in the reconstructed measurement information.
- The efficacy of the proposed metrology update algorithm, incorporating Doppler correction, is validated through simulation experiments. In contrast to traditional algorithms, the proposed algorithm proficiently mitigates the issue of cumulative errors in angle measurements, thereby elevating the precision of localization.

The remainder of this paper is organized as follows. The underwater positioning model without latency and EKF nonlinear filtering method are introduced in Section 2. Section 3 presents the compensation algorithm based on measurement update and the Doppler correction method, The simulation results are analyzed in Section 4. The conclusions and future works are presented in Section 5.

2. Underwater Positioning Methods

In practical applications, AUVs are typically equipped with highly accurate depth sensors, because given that the depth information of underwater vehicles tends not to undergo abrupt changes, the influence of depth information can be momentarily disregarded in the navigation and localization systems outlined in this study. Consequently, three-dimensional spatial localization can be simplified into a two-dimensional plane localization problem. The formulas in this chapter are referenced from the literature [41].

2.1. Positioning Model without Latency

To solve the AUV localization problem, we establish a northeast ground localization coordinate system. To illustrate the localization problem more conveniently, in this thesis, we consider the use of only one observatory node and one AUV. The AUV motion model is shown in Figure 1. We assume that the initial position of the observatory is known and set as (x_0, y_0). By creating a two-dimensional discrete-time model with sampling interval T_s, the real-time estimation of the AUV's position at time t_k can be described using the following state information:

$$\begin{cases} x_k = x_{k-1} + v_{k-1} T_s \cos \varphi_{k-1} \\ y_k = y_{k-1} + v_{k-1} T_s \sin \varphi_{k-1} \\ \varphi_k = \varphi_{k-1} + \omega_{k-1} T_s \end{cases} \tag{1}$$

where x_k, y_k, and v_k denote the positional coordinates of the AUV at time t_k and the forward travel speed, respectively. φ_k denotes the heading angle, ω_k denotes the angular velocity of the heading, and T_s denotes the sampling interval of the sensor.

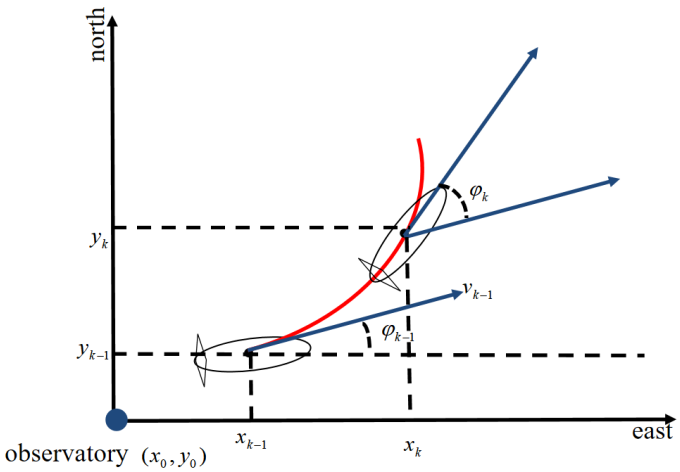

Figure 1. AUV motion model.

The position of the AUV is influenced by system inputs v_k and ω_k, and system inputs u_k are

$$u_k = \begin{bmatrix} v_k - w_{vk} \\ \omega_k - w_{\omega k} \end{bmatrix} = \begin{bmatrix} v_k \\ \omega_k \end{bmatrix} - w_k \tag{2}$$

where w_{vk} denotes the zero-mean Gaussian white noise of the forward velocity and $w_{\omega k}$ denotes the zero-mean Gaussian white noise of the angular velocity of the heading.

Within the navigation coordinate system, the AUV's position is characterized by components along both the x- and y-axes. The dynamic state variables encompass x-, y-, and forward-heading angles φ_k. The position information and heading angle in the coordinate system are selected as the system state quantities X. The system state of the AUV at time t_k is defined as X_k, and the state quantity of the system is

$$X_{\mathrm{k}} = [x_k \;\; \mathrm{y}_k \;\; \varphi_k]^T \tag{3}$$

The AUV's x-coordinate is the sum of its previous x-coordinate and x-axis projection of the distance covered during the time interval. Specifically, the AUV traverses a distance of $v * t_s$ in each time segment projected as $v * t_s * \cos(\varphi)$ on the x-aixs. The y coordinates follow a similar principle. The angle is derived by integrating the angular velocity at each moment. Consequently, referring to Equation (1), the state equation of the system can be expressed as

$$X_{\mathrm{k}} = f(X_{k-1}, u_{k-1}) \tag{4}$$

In a real underwater sports environment, an observatory detects and localizes the AUV for tracking purposes. The relative distance information between the observatory and the AUV is integrated into the EKF process as observation data for correction. Assuming that the observatory coordinates are $\left(x_k^M, y_k^M\right)$, the relative distance is calculated as follows:

$$d_k = \sqrt{\left(x_k - x_k^M\right)^2 + \left(y_k - y_k^M\right)^2} \tag{5}$$

Taking d_k as the observation information of the system, the observation equation of the system is

$$\mathrm{z}_k = \sqrt{\left(x_k - x_k^M\right)^2 + \left(y_k - y_k^M\right)^2} + \psi_k^p \tag{6}$$

where ψ_k^p denotes the observation noise of the system.

Based on the information provided, the nonlinear model of the system in the discrete-time state space is expressed as

$$\begin{cases} X_{\mathrm{k}} = f(X_{k-1}, u_{k-1}) + \Gamma_{k-1} W_{\mathrm{k}} \\ \mathrm{z}_k = \left(x_k - x_k^M\right)^2 + \left(y_k - y_k^M\right)^2 + \psi_k^p \end{cases} \tag{7}$$

where Γ_{k-1} denotes the system noise transfer matrix and W_{k} denotes the system process noise.

2.2. Extended Kalman Filter Estimation

Based on the system state model established in the previous section, it is evident that both the state and observation equations of the system incorporate nonlinear terms, rendering the conventional KF algorithm unsuitable. A typical approach to filtering problems within nonlinear systems involves transforming them into approximate linear filtering problems using linearization techniques. Among these, the EKF method is the most extensive method. The fundamental concept is as follows: In the case of a typical nonlinear system, the nonlinear functions $f(*)$ and $h(*)$ are initially expanded into a Taylor series around the filter's value $\hat{X}_k$, with the omission of second-order and higher-order terms to yield an approximately linearized model. Subsequently, a Kalman Filter is employed to accomplish filtering and estimation of the target.

The precise steps for the estimation employing the Extended Kalman Filter are as follows:

Step 1: State Prediction

$$\hat{X}_{k|k-1} = f(\hat{X}_{k-1}, u_{k-1}) \tag{8}$$

Step 2: Observation Prediction

$$\hat{Z}_{k|k-1} = h(\hat{X}_{k|k-1}) \tag{9}$$

Step 3: Linearize the state equation. According to Equation (4), taking the partial derivative of $f(*)$ with respect to $\hat{X}_{k-1}$, we obtain the Jacobian matrix with respect to $\hat{X}_{k-1}$, denoted as the state transition matrix Φ_k, which expands as follows:

$$\Phi_{k|k-1} = \frac{\partial f}{\partial X_{K-1}}\bigg|_{X_{K-1}=\hat{X}_{k-1}} = \begin{bmatrix} 1 & 0 & -v_{k-1}T_s \sin\varphi_{k-1} \\ 0 & 1 & v_{k-1}T_s \cos\varphi_{k-1} \\ 0 & 0 & 1 \end{bmatrix}$$

$$\Gamma_{k-1} = \frac{\partial f}{\partial u_{k-1}}\big|_{u_{k-1}=\hat{u}_{k-1}} = \begin{bmatrix} T_s \cos\varphi_{k-1} & 0 \\ T_s \sin\varphi_{k-1} & 0 \\ 0 & T_s \end{bmatrix}$$

Step 4: Linearize the observation equation. According to Equation (6), taking the partial derivative of $h(*)$ with respect to $\hat{X}_{k|k-1}$, we obtain a Jacobian matrix with respect to $\hat{X}_{k|k-1}$, denoted by the state transition matrix H_k, which is expanded as follows:

$$H_k = \left[\frac{x_k - x_k^M}{\sqrt{(x_k - x_k^M)^2 + (y_k - y_k^M)^2}}, \frac{y_k - y_k^M}{\sqrt{(x_k - x_k^M)^2 + (y_k - y_k^M)^2}}, 0 \right] \tag{10}$$

Step 5: Calculate covariance matrix.

$$P_{k|k-1} = \Phi_{k|k-1} P_{k-1} \Phi_{k|k-1}^T + \Gamma_{k-1} Q_{k-1} \Gamma_{k-1}^T \tag{11}$$

Step 6: Calculate Kalman gain.

$$K_k = P_{k|k-1} H_k^T (H_k P_{k|k-1} H_k^T + R_k)^{-1} \tag{12}$$

Step 7: State update.

$$\hat{X}_k = \hat{X}_{k|k-1} + K_k(Z_k - \hat{Z}_{k|k-1}) \tag{13}$$

Step 8: Covariance update.

$$P_k = (I - K_k H_k) P_{k|k-1} \tag{14}$$

This constitutes the computational cycle of EKF. The treatment of nonlinear systems using EKF involves the continuous iterations of the computational cycle. Within this iterative process, the AUV receives range information from the observatory, integrates it into the EKF update process, and consequently acquires the position information to continuously refine its position.

3. Communication Delay Compensation Algorithm

AUVs are used in complex marine environments, where their navigation and positioning can be affected by harsh conditions and the instability of measurement sensors, leading to unknown system noise, and thereby, resulting in unknown measurement system errors [42]. For instance, mutual communication between the AUV and the observatory is a fundamental requirement for achieving navigation and positioning based on distance information. However, owing to the AUV's operation in underwater environments, signal transmission naturally incurs a certain amount of time delay. Consequently, there is an inevitable time lag in the relative positioning information transmitted from the observatory

to the AUV. The impact of the signal transmission delay on navigation performance is often a factor that cannot be overlooked. The communication delay between the AUV and navigation system of the observatory is illustrated in Figure 2. The observatory transmits distance information to the AUV at time moment t_1; however, the AUV receives the communication signal at time moment t_2 with time $\delta_t = t_2 - t_1$. During this period, the AUV's position can change with in relation to time t_1. If range information is incorporated into the filter for measurement and updating, then a substantial error may be introduced, adversely affecting the navigation performance.

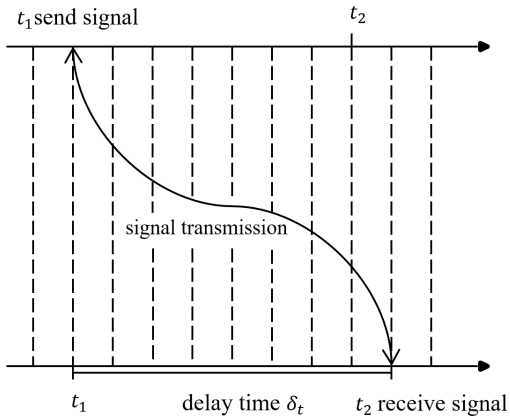

Figure 2. Positioning system communication delay schematic.

3.1. Compensation Algorithm Based on Measurement Update

In response to the communication delay problem in AUV underwater localization, a time delay is introduced into the measurement equation of EKF, and the optimal state estimation is deduced according to the principle of minimum variance estimation [38].

The relative motion between the AUV and observatory is depicted in Figure 3. Assuming that at time t_1, the coordinates of the observation station are represented by $P_1^M = (x_1^M, y_1^M)$, and the AUV's position coordinates are denoted as $p_1 = (x_1, y_1)$, the observed distance between the AUV and the observation station at this moment is d_1. At time t_2, the AUV's position coordinates, denoted as $p_2 = (x_2, y_2)$, are obtained after the AUV has moved for a duration of δ_t. The observed distance between the AUV and the observation station is d_2. According to Equation (5), we can calculate the values of d_1 and d_2, as illustrated in Equation (15).

$$\begin{cases} d_1 = \sqrt{(x_1 - x_1^M)^2 + (y_1 - y_1^M)^2} \\ d_2 = \sqrt{(x_2 - x_1^M)^2 + (y_2 - y_1^M)^2} \end{cases} \tag{15}$$

From Figure 3, we can infer that due to the presence of delays, when computing the measurement information of the AUV at time t_1, the AUV has already moved from p_1 to p_2. At this point, the obtained measurement information is no longer accurate, and Equation (5) is no longer applicable. To address this issue, it is necessary to reconstruct the measurement equation to obtain more accurate measurement information. Assuming that the AUV maintains a constant speed during the communication delay δ_t, it covers a distance represented by $d_{\delta t} = v_2 \delta_t$. Based on the AUV's position at the moment of signal reception t_2, we can calculate and infer its position at time t_1. The coordinates of this inferred position can be denoted as $P_1' = (x_1' \; y_1')$, which fulfills the following equation:

$$\begin{cases} x_1' = x_2 - d_{\delta t} \cos \varphi_2 \\ y_1' = y_2 - d_{\delta t} \sin \varphi_2 \end{cases} \tag{16}$$

The relative distance between P_1' and the observatory is expressed as

$$d_1' = \sqrt{\left(x_1' - x_1^M\right)^2 + \left(y_1' - y_1^M\right)^2} \tag{17}$$

As depicted in Figure 3, we deduce that $\beta = \alpha + \varphi$. The relative azimuth between the station and AUV at time t_1 is as follows:

$$\alpha = \arctan\left(\frac{x_1' - x_1^M}{y_1' - y_1^M}\right) \tag{18}$$

The reconstituted measurement data are as follows:

$$Z_k = {d_1'}^2 + d_{\delta t}^2 - 2{d_1'}^2 d_{\delta t}^2 \cos\beta \tag{19}$$

Subsequently, the reconstructed measurement information undergoes a measurement update within the filter. Through the acquisition of more precise relative positional information at time t_2, this method compensates for communication delay-induced positioning errors. Additionally, this approach reconstructs the measurement equation on the foundation of EKF, thereby obviating the necessity for extra data storage and computational resources.

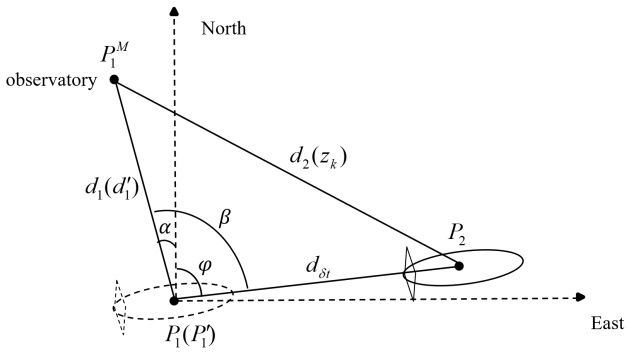

Figure 3. AUV movement schematic.

3.2. Doppler Correction

3.2.1. Usability Analysis

In practical application environments, the velocity information obtained from the AUV's own sensors is already relatively accurate, while the angles, influenced by the underwater environment, can lead to positioning errors. The Doppler Velocity Log (DVL) is a commonly used acoustic velocity measurement instrument that can measure the velocity of the carrier in real time [43]. The navigation method based on the Doppler effect has the advantage that the navigation error does not increase cumulatively [44]. Based on this characteristic, we can rectify the angles of the AUV.

From Equation (19), it can be observed that the new measurement information equation relies on the calculation of angle β; nevertheless, the sensor's own positional data are subject to noise-induced errors. Indeed, when the sensor follows a curved trajectory, the azimuth angles undergo continuous variation. In such circumstances, the aforementioned methods are prone to error accumulation, thus adversely affecting the positioning accuracy. In response to the aforementioned challenges, a Doppler measurement model is proposed. This model calculates the relative angles based on the received frequency variations, thereby effectively alleviating the problem of error accumulation and enhancing the positioning precision.

The geometry for the mobile sensor localization based on the Doppler measurement model is shown in Figure 4. Assuming that the AUV has M motion trajectory segments and the sensor is moving at a constant velocity at the mth trajectory segment, $m = 1, 2, ..., M$, and kth sampling point, $k = 1, 2, ...k_m$, the position of the AUV is denoted as $s_{m,k} =$

$[s_{x,m,k}, s_{y,m,k}, s_{z,m,k}]^T$, velocity is denoted as $v_{m,k} = [v_{x,m,k}, v_{y,m,k}, v_{z,m,k}]^T$, and the coordinates of the location of the observatory are denoted as $u = [u_x, u_y, u_z]^T$.

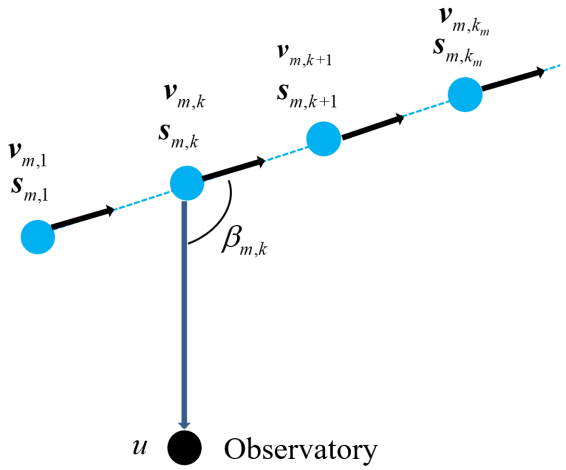

Figure 4. Geometry of localization based on Doppler measurements.

The Doppler measurement equations are given by Equation (20):

$$\begin{cases} \tilde{f}_{m,k} = f_{m,k} + e_{m,k} \\ f_{m,k} = f_s\left(1 + \frac{v_{m,k}^T(u - s_{m,k})}{c\|u - s_{m,k}\|}\right) = f_s\left(1 + \frac{\|v_{m,k}\|}{c}\cos\beta_{m,k}\right) \end{cases} \tag{20}$$

where f_s denotes the frequency of the acoustic signal emitted by the target, c denotes the speed at which the signal propagates through the water, and $e_{m,k} \sim N(0,\ \sigma_{m,k}^2)$ is an independent Gaussian white noise with zero mean and $\sigma_{m,k}^2$ variance, β denotes the angle between the direction vector $d_{m,k} = u - s_{m,k}$ of the AUV to the observatory and velocity vector $v_{m,k}$ of the AUV.

3.2.2. Analysis of the Doppler Correction Algorithm

In this experimental environment, it is assumed that the depth information will not change in a short period of time, ignoring the influence of the depth information. Therefore, we exclusively focus on positional data along the northeast direction, effectively reducing the three-dimensional problem to a two-dimensional one. The trajectory of the AUV is characterized by a curve. Consequently, Equation (20) can be reformulated as

$$\begin{cases} \tilde{f}_k = f_k + e_k \\ f_k = f_s\left(1 + \frac{v_k^T(u - s_k)}{c|u - s_k|}\right) = f_s\left(1 + \frac{|v_k|}{c}\cos\beta_k\right) \end{cases} \tag{21}$$

From Equation (21), the angle β_k obtained through Doppler frequency shift measurement is

$$\beta_k = \arccos\left(\frac{c}{|v_k|}\left(\frac{f_k}{f_s} - 1\right)\right) \tag{22}$$

Substituting β_k into Equation (19), the updated measurement data are presented in Equation (23).

$$Z_k' = {d_1'}^2 + d_{\delta t}^2 - 2{d_1'}^2 d_{\delta t}^2 \cos\beta_k \tag{23}$$

Ultimately, the updated measurement data are introduced into the filter for measurement updating, leading to the acquisition of position-estimation information that appropriately compensates for the delay. The proposed algorithm for position estimation based on Doppler-corrected angles is illustrated in Algorithm 1.

Algorithm 1 Position estimation based on Doppler-corrected angles

Initialize parameters: $\beta_0, c, v_0, X_0, Z_0, Xn_0, Z\_update_0$
for $i = 1 : N$ **do**
    // State equation;
    $X_i = f(X_{i-1}, u_{i-1}) + \omega_{i-1})$;
    // Observation equation.;
    $Z_i = h(X_i) + V_i$
end for
// Doppler correction
for $i = 1 : N$ **do**
    $\beta_i = \arccos(\frac{c}{v_i}(\frac{f_k^i}{f_s} - 1))$;
end for;
// EKF
for $i = 1 : N$ **do**
    // State Prediction;
    $Xn_i = f(Xn_{i-1}, un_{i-1})$
    // Measurement information update;
    $Z\_update_i = {d'_i}^2 + d_{\delta t}^2 - 2{d'_i}^2 d_{\delta t}^2 \cos\beta_i$
    // State update;
    $X\_ekf_i = Xn_i + K_i(Z\_update_i - Z_i)$
end for

4. Simulation

When the AUV travels in a consistent direction, the limited variation in its heading angle leads to an inconsequential cumulative angular error. Consequently, the optimization impact of the proposed method is comparatively modest when contrasted with EKF and measurement update methods. When the sensor follows a curved trajectory, the azimuth angles undergo continuous variation. In this scenario, the outcomes of the proposed method exhibit a more favorable comparison in contrast to the aforementioned methods. Therefore, simulation experiments are conducted with the AUV trajectories defined as curves to more comprehensively elucidate the efficacy of the proposed method.

We assume a sensor system noise level of $\sigma_v = 0.1$ m/s, a communication delay time of $\delta_t = 1$ s, a curved trajectory for the sensor, an angular velocity of 0.01°/s during its movement, and an airspeed of 3 m/s. The initial simulation parameters can be summarized in Table 1.

Table 1. The initial simulation parameters

Parameters	Value	Meaning
δ_t	1s	Communication latency
ω	0.01°/s	Angular velocity
v	3 m/s	AUV travel speed
c	1500 m/s	Underwater sound wave propagation speed
f_s	10 kHZ	Doppler emission frequency
σ_v	/	System noise
e_k	/	Doppler observation noise

The Root Mean Squared Error (RMSE) of 100 Monte Carlo simulation experiments was calculated, and the RMSE calculation formula is shown in Equation (24).

$$RMSE : \tilde{x}_k^i = \sqrt{\frac{1}{M}\sum_{j=1}^{M}[\tilde{x}_k^i(j)]^2} \tag{24}$$

where $\tilde{x}_k^i(j)$ is the estimation error of ith state variable in the jth simulation, $j = 1, 2...M$, $M = 100$ and $\tilde{x}_k^i$ is the RMSE of the ith state variable.

The proposed Doppler-updating algorithm is compared with the EKF and measurement-updating EKF algorithms in Equation (19), and the simulation results are shown in Figures 5–11. The results of the average error of 100 experiments are presented in Table 2. We have conducted an analysis of the statistical data in Table 2, calculating the arithmetic mean and SD (standard deviation). Furthermore, we have performed a comparative analysis of the localization performance of three algorithms, and the results are presented in Table 3. The results reveal that the incorporation of Doppler angle correction in the reconstructed measurement information method significantly decreases the localization error by approximately 50% compared to EKF and by around 20% compared to the method lacking angle correction. The data obtained from 100 repeated experiments reveal that the proposed algorithm exhibits the smallest SD, indicating the most stable performance.

From Figures 5 and 6, we can observe the motion trend of the AUV by employing different algorithms and also the trend of RMSE of the heading angle. In the initial phase, the AUV maintains a relatively constant heading angle, follows a trajectory closely resembling a straight line, and aligns well with the actual trajectory. During the curve-driving phase, the AUV exhibits increased variability in the heading angle, leading to more apparent deviations among the three trajectories. Notably, the trajectory employing the Doppler angle correction method exhibits the closest alignment with the real trajectory.

Table 2. Average error of 100 experiments.

Simulation		EKF	Measurement Updating	Doppler Updating
1th	Average error/(m)	0.4768	2.2733	1.4456
2th	Average error/(m)	1.5151	1.2834	1.5445
3th	Average error/(m)	3.6834	1.6826	1.592
4th	Average error/(m)	2.7569	2.2994	1.3056
5th	Average error/(m)	1.1705	1.9486	1.4824
6th	Average error/(m)	1.4215	2.2187	1.3861
7th	Average error/(m)	5.4215	1.9356	1.8949
8th	Average error/(m)	0.43878	2.4597	1.3958
9th	Average error/(m)	3.6829	1.4322	1.634
10th	Average error/(m)	5.1604	2.0432	1.5967
...	...	...	...	...
98th	Average error/(m)	1.202	1.8476	1.4613
99th	Average error/(m)	2.6694	2.0432	1.4002
100th	Average error/(m)	1.2106	2.3533	1.5146

Table 3. Analysis of statistical data.

	EKF	Measurement Updating	Doppler Updating
Mean of 100 experiments	2.6167	2.0425	1.475
SD	2.0824	0.468	0.1208
Comparison of errors	100%	78.06%	56.37%

The root cause of this outcome lies in the AUV's underwater curved motion, where the EKF algorithm's observational data are prone to substantial inaccuracies due to waterborne acoustic communication delays. While the measurement-update approach addresses these delays, it introduces cumulative angle errors into the positional estimation process. In contrast, the Doppler update method, being more responsive to angle-information measurements, yields relatively small errors, effectively mitigating the accumulation of angle-related discrepancies.

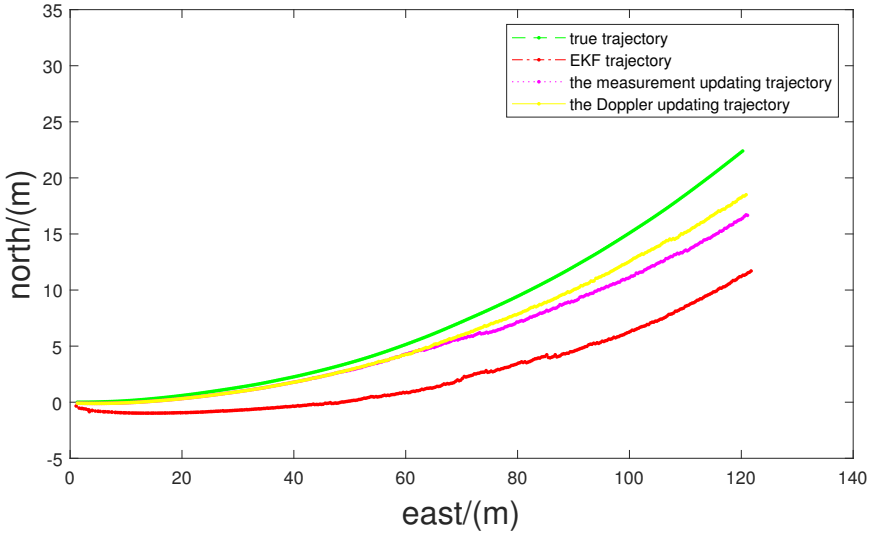

Figure 5. AUV trajectory.

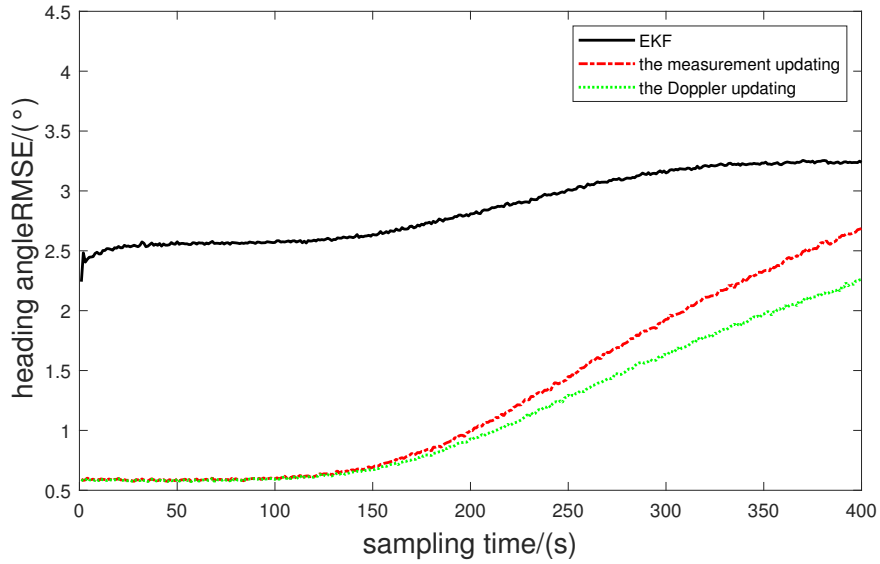

Figure 6. RMSE of heading position.

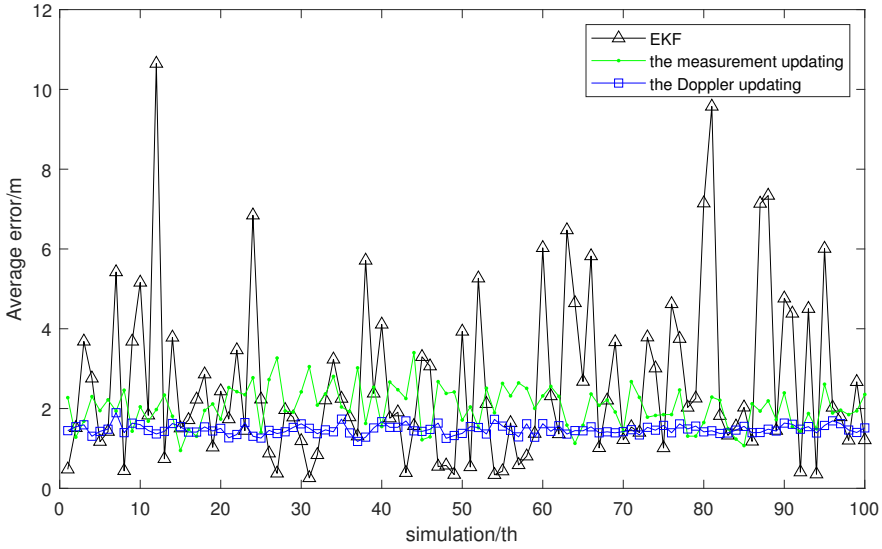

Figure 7. Average error of 100 experiments.

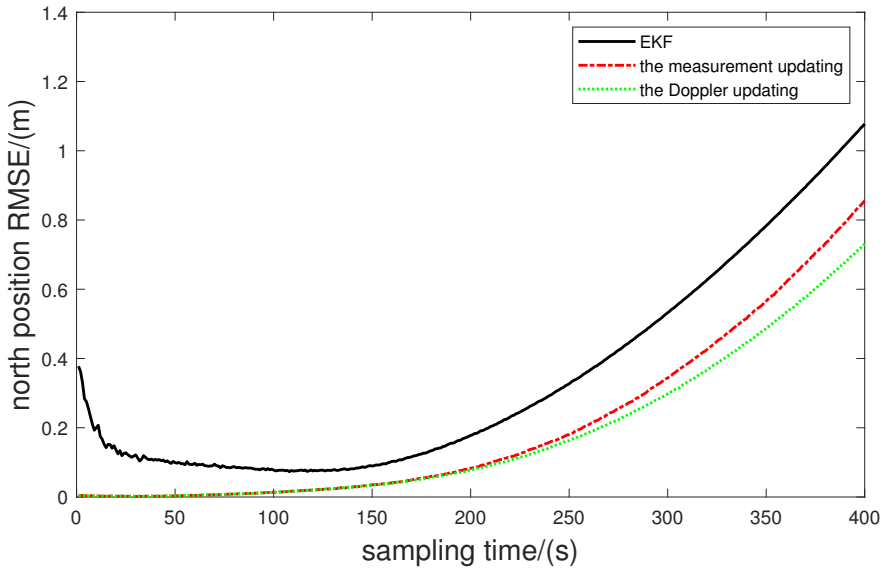

Figure 8. RMSE of north position.

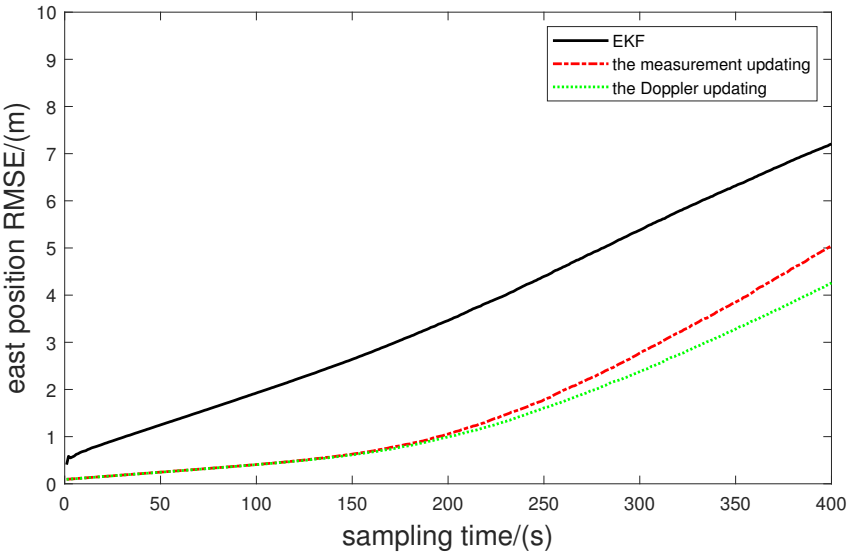

Figure 9. RMSE of east position.

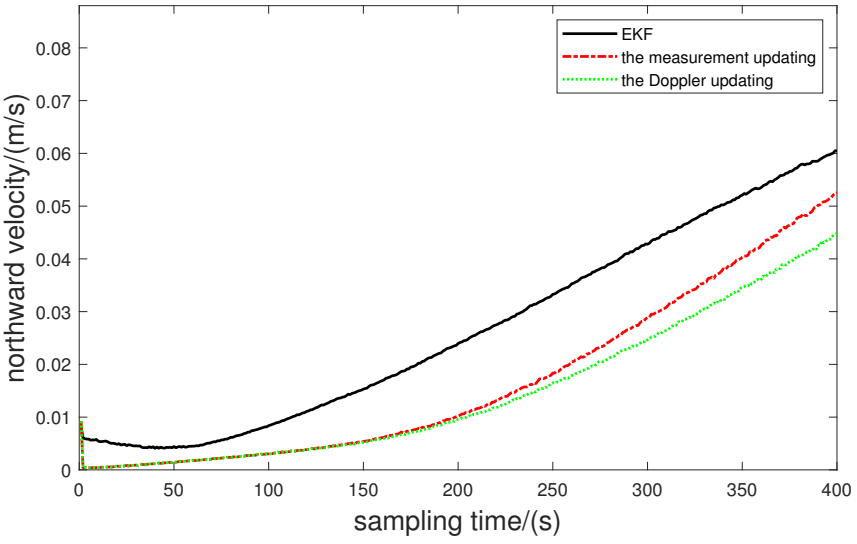

Figure 10. RMSE of northward velocity.

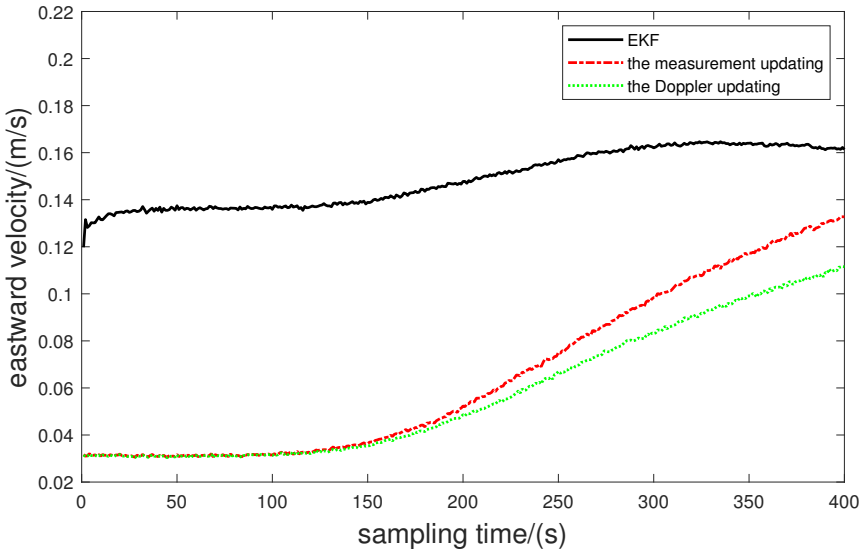

Figure 11. RMSE of eastward velocity.

From Figure 7, it is evident that in the 100 repeated experiments, EKF exhibits considerable fluctuations. In comparison, the measurement updating algorithm demonstrates relatively lower volatility, while the Doppler updating algorithm displays the minimal fluctuations, indicating the most stable performance.

From Figures 8–11, the Doppler updating method, designed to mitigate underwater communication delays and cumulative angular errors, results in an RMSE slightly inferior to that of the measurement updating algorithm. However, both these methods significantly outperform the EKF. This observation underscores the enhanced suitability of the proposed Doppler-updating algorithm for intricate localization scenarios, ultimately yielding more optimal results.

5. Conclusions

To address the challenge of reduced positioning accuracy resulting from communication delays in underwater positioning environments, an enhanced EKF filtering technique is proposed. This approach leverages reconstructed measurement data and introduces Doppler measurements for angular correction within the framework of a range-based navigation model. The combination of these elements refines the EKF filtering method. This method establishes a relationship between the measurement data before and after the delay based on the current motion state of the AUV. Subsequently, it reconstructs fresh measurement data and rectifies angle-related inaccuracies using Doppler measurements. This approach mitigates error accumulation and enhances the precision of the positioning system. The simulation results confirm the effectiveness of this technique in compensating for positioning errors induced by communication delays in underwater navigation, ultimately elevating the AUV positioning accuracy. This paper holds substantial significance in tackling the challenges posed by delayed impact, intricate localization, and the high costs linked with AUV. A critical facet for resolving AUV positioning issues lies in compensating for localization errors through the reconstruction of measurement information.

In the future, we will consider the problem of cooperative positioning of multiple AUVs, which will be further realized by the master-slave cooperative positioning model to improve the accuracy of cooperative positioning. In addition, the AUV cluster control problem will also be considered for AUV cooperative formation, which is more in line with the operation in real underwater environments.

Author Contributions: Conceptualization, P.L. and Z.L.; methodology, Z.L.; software, J.C.; validation, P.L., Z.L. and C.C.; formal analysis, C.C.; investigation, P.L., Z.L. and J.C.; data curation, P.L. and Z.L.; writing—review and editing, Z.L. and Z.C.; visualization, Z.L.; project administration, C.C., P.L. and Z.C.; funding acquisition, C.C., P.L. and Z.C. All authors have read and agreed to the published version of the manuscript.

Funding: This research was funded by the National Key R&D Program of China for International S&T Cooperation Projects (2019YFE0118700), National Natural Science Foundation of China (62222306, 62203165), Research Foundation of Education Bureau of Hunan Province, China (21B0456) and Shenzhen Fundamental Research (JCYJ20210324101215039).

Data Availability Statement: Data are contained within the article.

Conflicts of Interest: The authors declare no conflict of interest.

References

1. Paull, L.; Saeedi, S.; Seto, M.; Li, H. AUV navigation and localization: A review. *IEEE J. Ocean. Eng.* **2013**, *39*, 131–149. [CrossRef]
2. Wakita, N.; Hirokawa, K.; Ichikawa, T.; Yamauchi, Y. Development of autonomous underwater vehicle (AUV) for exploring deep sea marine mineral resources. *Mitsubishi Heavy Ind. Tech. Rev.* **2010**, *47*, 73–80.
3. Wang, Y.; Gu, D.; Ma, X.; Wang, J.; Wang, H. Robust Real-Time AUV Self-Localization Based on Stereo Vision-Inertia. *IEEE Trans. Veh. Technol.* **2023**, *72*, 7160–7170. [CrossRef]
4. Guo, J.; Li, D.; He, B. Intelligent collaborative navigation and control for AUV tracking. *IEEE Trans. Ind. Inform.* **2020**, *17*, 1732–1741. [CrossRef]
5. Kepper, J.H.; Claus, B.C.; Kinsey, J.C. A navigation solution using a MEMS IMU, model-based dead-reckoning, and one-way-travel-time acoustic range measurements for autonomous underwater vehicles. *IEEE J. Ocean. Eng.* **2018**, *44*, 664–682. [CrossRef]
6. Stojanovic, M. Recent advances in high-speed underwater acoustic communications. *IEEE J. Ocean. Eng.* **1996**, *21*, 125–136. [CrossRef]
7. Chitre, M.; Shahabudeen, S.; Stojanovic, M. Underwater acoustic communications and networking: Recent advances and future challenges. *Mar. Technol. Soc. J.* **2008**, *42*, 103–116. [CrossRef]
8. Yang, G.; Dai, L.; Wei, Z. Challenges, threats, security issues and new trends of underwater wireless sensor networks. *Sensors* **2018**, *18*, 3907. [CrossRef]
9. Caiti, A.; Crisostomi, E.; Munafò, A. Physical characterization of acoustic communication channel properties in underwater mobile sensor networks. In Proceedings of the Sensor Systems and Software: First International ICST Conference, S-CUBE 2009, Pisa, Italy, 7–9 September 2009; Revised Selected Papers 1; Springer: Berlin, Germany, 2010; pp. 111–126.
10. Li, L.; Li, Y.; Zhang, Y.; Xu, G.; Zeng, J.; Feng, X. Formation Control of Multiple Autonomous Underwater Vehicles under Communication Delay, Packet Discreteness and Dropout. *J. Mar. Sci. Eng.* **2022**, *10*, 920. [CrossRef]
11. Zhou, L.; Wang, M.; Zhang, X.; Qin, P.; He, B. Adaptive SLAM Methodology Based on Simulated Annealing Particle Swarm Optimization for AUV Navigation. *Electronics* **2023**, *12*, 2372. [CrossRef]
12. Qu, J.; Sun, G.; Zhang, J.; Li, X.; Mao, Y.; Wang, J. Optimality analysis for formation of Multi-AUV cooperative positioning based on genetic algorithm. In Proceedings of the 2021 IEEE International Conference on Real-time Computing and Robotics (RCAR), Xining, China, 15–19 July 2021; pp. 578–583.
13. Ling, H.; Zhu, T.; He, W.; Zhang, Z.; Luo, H. Cooperative search method for multiple AUVs based on target clustering and path optimization. *Nat. Comput.* **2021**, *20*, 3–10. [CrossRef]
14. Lu, J.; Chen, X.; Luo, M.; Zhou, Y. Cooperative localization for multiple AUVs based on the rough estimation of the measurements. *Appl. Soft Comput.* **2020**, *91*, 106197. [CrossRef]
15. Chang, L.; Qin, F.; Xu, J. Strapdown inertial navigation system initial alignment based on group of double direct spatial isometries. *IEEE Sens. J.* **2021**, *22*, 803–818. [CrossRef]
16. Ji, D.X.; Fang, W.W.; Zhu, H.; Li, S.; Tang, Y.G.; Tian, Y.; Yao, Q. Active Localization of Autonomous Underwater Vehicle Using Noisy Relative Measurement. *Acta Electonica Sin.* **2021**, *49*, 1249.
17. Stutters, L.; Liu, H.; Tiltman, C.; Brown, D.J. Navigation Technologies for Autonomous Underwater Vehicles. *IEEE Trans. Syst. Man Cybern. Part C Appl. Rev.* **2008**, *38*, 581–589. [CrossRef]
18. Miller, P.A.; Farrell, J.A.; Zhao, Y.; Djapic, V. Autonomous Underwater Vehicle Navigation. *IEEE J. Ocean. Eng.* **2010**, *35*, 663–678. [CrossRef]
19. Du, C.; Li, F.; Shi, Y.; Yang, C.; Gui, W. Integral Event-Triggered Attack-Resilient Control of Aircraft-on-Ground Synergistic Turning System With Uncertain Tire Cornering Stiffness. *IEEE/CAA J. Autom. Sin.* **2023**, *10*, 1276–1287. [CrossRef]
20. Du, C.; Shi, Y.; Li, F.; Yang, C.; Gui, W. An Improved Co-Design Method of Dynamical Controller and Asynchronous Integral-Type Event-Triggered Mechanisms. *IEEE Trans. Syst. Man, Cybern. Syst.* **2023**, *53*, 2500–2509. [CrossRef]
21. Ji, D.; Deng, Z.; Li, S.; Ma, D.; Wang, T.; Song, W.; Zhu, S.; Wang, Z.; Pan, H.; Sharma, S.; et al. A Novel Case of Practical Exponential Observer Using Extended Kalman Filter. *IEEE Access* **2018**, *6*, 58004–58011. [CrossRef]

22. Hargrave, P. A tutorial introduction to Kalman Filtering. In Proceedings of the IEE Colloquium on Kalman Filters: Introduction, Applications and Future Developments, IET, London, UK, 21–21 February 1989; p. 1.
23. Xia, X.; Hashemi, E.; Xiong, L.; Khajepour, A. Autonomous vehicle kinematics and dynamics synthesis for sideslip angle estimation based on consensus Kalman Filter. *IEEE Trans. Control. Syst. Technol.* **2022**, *31*, 179–192. [CrossRef]
24. Xiong, L.; Xia, X.; Lu, Y.; Liu, W.; Gao, L.; Song, S.; Yu, Z. IMU-based automated vehicle body sideslip angle and attitude estimation aided by GNSS using parallel adaptive Kalman Filters. *IEEE Trans. Veh. Technol.* **2020**, *69*, 10668–10680. [CrossRef]
25. Liu, W.; Xia, X.; Xiong, L.; Lu, Y.; Gao, L.; Yu, Z. Automated vehicle sideslip angle estimation considering signal measurement characteristic. *IEEE Sens. J.* **2021**, *21*, 21675–21687. [CrossRef]
26. Xia, X.; Xiong, L.; Huang, Y.; Lu, Y.; Gao, L.; Xu, N.; Yu, Z. Estimation on IMU yaw misalignment by fusing information of automotive onboard sensors. *Mech. Syst. Signal Process.* **2022**, *162*, 107993. [CrossRef]
27. Zhang, X.; Mu, X.; Liu, H.; He, B.; Yan, T. Application of modified ekf based on intelligent data fusion in auv navigation. In Proceedings of the 2019 IEEE Underwater Technology (UT), Kaohsiung, Taiwan, 16–19 April 2019; pp. 1–4.
28. Mao, G.; Drake, S.; Anderson, B.D. Design of an extended Kalman Filter for uav localization. In Proceedings of the 2007 Information, Decision and Control, Adelaide, Australia, 12–14 February 2007; pp. 224–229.
29. Huang, Y.; Zhang, Y.; Xu, B.; Wu, Z.; Chambers, J.A. A New Adaptive Extended Kalman Filter for Cooperative Localization. *IEEE Trans. Aerosp. Electron. Syst.* **2018**, *54*, 353–368. [CrossRef]
30. Petroni, A.; Scarano, G.; Cusani, R.; Biagi, M. On the Effect of Channel Knowledge in Underwater Acoustic Communications: Estimation, Prediction and Protocol. *Electronics* **2023**, *12*, 1552. [CrossRef]
31. Wang, Y.; Zhang, X.; Sun, S.; Wang, J. Underwater navigation using a single beacon based on the time delays of the direct signals and the surface-reflected signals. *Appl. Acoust.* **2022**, *187*, 108503. [CrossRef]
32. Xu, B.; Wang, X.; Guo, Y.; Zhang, J.; Razzaqi, A.A. A Novel Adaptive Filter for Cooperative Localization Under Time-Varying Delay and Non-Gaussian Noise. *IEEE Trans. Instrum. Meas.* **2021**, *70*, 9600615. [CrossRef]
33. Zhu, J.; Li, A.; Qin, F.; Che, H.; Wang, J. A Novel Hybrid Method Based on Deep Learning for an Integrated Navigation System during DVL Signal Failure. *Electronics* **2022**, *11*, 2980. [CrossRef]
34. Yan, J.; Gao, J.; Yang, X.; Luo, X.; Guan, X. Position tracking control of remotely operated underwater vehicles with communication delay. *IEEE Trans. Control. Syst. Technol.* **2019**, *28*, 2506–2514. [CrossRef]
35. Zhang, J.; Shi, C.; Sun, D.; Han, Y. High-precision, limited-beacon-aided AUV localization algorithm. *Ocean. Eng.* **2018**, *149*, 106–112. [CrossRef]
36. Li, Z.; Dosso, S.E.; Sun, D. Motion-Compensated Acoustic Localization for Underwater Vehicles. *IEEE J. Ocean. Eng.* **2016**, *41*, 840–851. [CrossRef]
37. Thomson, D.J.M.; Dosso, S.E.; Barclay, D.R. Modeling AUV Localization Error in a Long Baseline Acoustic Positioning System. *IEEE J. Ocean. Eng.* **2017**, *43*, 955–968. [CrossRef]
38. Xu, B.; Qiu, L.; Yang, J. Analysis of time delay and error compensation for multi-AUVs cooperative navigation approach. *Control. Decis.* **2015**, *30*, 9–16.
39. Yao, Y.; Xu, D.; Yan, W. Cooperative localization with communication delays for MAUVs. In Proceedings of the 2009 IEEE International Conference on Intelligent Computing and Intelligent Systems, Shanghai, China, 20–22 November 2009; Volume 1, pp. 244–249.
40. Yao, Y.; Xu, D.; Zhang, L.; Yan, W. Cooperative localization of multiple UUVs with communication delays- A real-time update method based on path prediction. *Robot* **2011**, *33*, 161–168. [CrossRef]
41. Wang, W.-j.; Sun, R.-z.; Gao, W.; Xu, B. Cooperative navigation based on error compensation of communication delays. *Fire Control Command. Control* **2014**, *39*, 27–30.
42. Sheng, G.; Liu, X.; Sheng, Y.; Cheng, X.; Luo, H. Cooperative Navigation Algorithm of Extended Kalman Filter Based on Combined Observation for AUVs. *Remote Sens.* **2023**, *15*, 533. [CrossRef]
43. Wang, Q.; Liu, K.; Cao, Z. System noise variance matrix adaptive Kalman Filter method for AUV INS/DVL navigation system. *Ocean. Eng.* **2023**, *267*, 113269. [CrossRef]
44. Morgado, M.; Oliveira, P.; Silvestre, C. Tightly coupled ultrashort baseline and inertial navigation system for underwater vehicles: An experimental validation. *J. Field Robot.* **2013**, *30*, 142–170. [CrossRef]